Article

Leaf proteomic analysis in two maize landraces with different tolerance to boron toxicity

Betty M. Mamani-Huarcaya[1,2], M. Teresa Navarro-Gochicoa[1], M. Begoña Herrera-Rodríguez[1], Juan J. Camacho-Cristóbal[1], Carlos J. Ceacero[1], Óscar Fernández Cutire[3], Agustín González-Fontes[1] and Jesús Rexach[1,*]

[1] Departamento de Fisiología, Anatomía y Biología Celular, Universidad Pablo de Olavide, E-41013 Sevilla, Spain; jrexben@upo.es
[2] Laboratorio de Biotecnología Vegetal, Escuela de Agronomía, Facultad Ciencias Agropecuarias, Universidad Nacional Jorge Basadre Grohmann, Tacna, Perú
[3] Departamento de Agronomía, Facultad Ciencias Agropecuarias, Universidad Nacional Jorge Basadre Grohmann, Tacna, Perú
* Correspondence: jrexben@upo.es

Abstract: Boron (B) toxicity is an important stress that negatively affects maize yield and quality production. The excessive B content in agricultural lands is a growing problem due to the increase in arid and semi-arid areas because of climate change. Recently, two Peruvian maize landraces, Sama and Pachía, were physiologically characterized based on their tolerance to B toxicity, the former being more tolerant to B excess than Pachía. However, many aspects regarding the molecular mechanisms of these two maize landraces against B toxicity are still unknown. In this study, a leaf proteomic analysis of Sama and Pachía was performed. Out of a total of 2793 proteins identified only 303 proteins were differentially accumulated. Functional analysis indicated that many of these proteins are involved in transcription and translation processes, amino acids metabolism, photosynthesis, carbohydrate metabolism, protein degradation, and protein stabilization and folding. Compared to Sama, Pachía had a higher number of differentially expressed proteins related to protein degradation, and transcription and translation processes under B toxicity conditions, which might reflect the greater protein damage caused by B toxicity in Pachía. Our results suggest that higher tolerance to B toxicity of Sama can be attributed to more stable photosynthesis that would avoid damage caused by stromal over-reduction under this stress condition.

Keywords: boron toxicity; proteomic analysis; maize landrace; *Zea mays*

1. Introduction

Boron (B) is an essential element for plants being well known its structural role in both cell walls and membranes [1-5]. Actually, B establishes diester bonds between apiose residues of two rhamnogalacturonan-II (RGII) molecules forming RGII-B complexes that stabilize the pectin network of the cell wall [6-8]. Furthermore, B contributes to the preservation of plasmalemma integrity and function [9], likely through the formation of B complexes with membrane components that contain *cis*-diol groups [10,11]. Thereby, B forms complexes with major constituents of membrane lipid rafts, such a as glycosyl inositol phosphoryl ceramides (GIPCs) [12]. Moreover, B participates in the formation of GIPCs-B-RGII complexes, which connect the plasmalemma to the cell wall [13]. Besides these structural roles, B is also involved in plant development participating in root and shoot elongation, pollen-tube growth, flowering, and fruiting [14-16]. In addition, B has been reported to participate in several physiological processes, such as photosynthesis, nucleic acid synthesis, phenolic, nitrogen and polyamines metabolisms, proteins stabilization and biosynthesis, and gene expression, among others [16-22].

Since B is a micronutrient, the range between its deficient, optimal, and toxic concentrations for plants is very narrow [23]. Therefore, it is common to find soils with inadequate B content for optimal plant development. Soils with high B contents predominantly occurs in arid and semi-arid countries,

 doi:10.20944/preprints202305.0301.v1

where this micronutrient accumulates in the topsoil mainly owing to high evapotranspiration and tiny leaching caused by low rainfall, a situation that is often aggravated by irrigation with B-enriched water [22,23]. Additionally, excess B is also found in lands close to coastal areas due to the hydraulic connection between their coastal aquifers and seawater [24] or in regions with recurrent geothermal activities [2]. Climate change is another factor that is contributing to the B increase in soils. Increasing temperatures and decreasing rainfall are predicted in the coming years, which will lead to an increase in agricultural areas with excessive B levels [3,25].

Excessive B contents in soils cause adverse effects such as chlorosis and necrosis in leaves, damages to stems and buds, and misshapen fruits [17,22]. Furthermore, an excess of B provokes DNA damages, inhibition of protein folding, impairment of protein functions and activities, and alterations in photosynthesis and nitrogen and carbon metabolisms, among other processes [2,22,26]. In fact, several photosynthetic parameters, such as CO_2 assimilation (P_N), photosynthetic electron transport rate (ETR), maximum quantum yield of chlorophyll fluorescence (Fv/Fm), and CO_2 use efficiency decreased under B toxicity conditions [22,27]. Because of the aforementioned effects of B toxicity in plant physiology, elevated B contents in agricultural lands reduce crop growth, yield, and quality [22,28]. In fact, a noteworthy decrease in the yield of several main crops subjected to B toxicity has been reported [28]. Despite the large number of effects caused by B toxicity in plants, it is not well known how B produces these alterations. However, it has been suggested that the ability of B to form bonds with molecules containing mono-, di- and poly-hydroxyl groups could be the chemical basis by which B toxicity could trigger morphophysiological alterations [29].

Maize is an important crop that provides approximately half of the calories consumed worldwide being, in addition, one of the principal genetic model plants for crop improvement and food security [30-32]. However, maize production is seriously constrained by abiotic and biotic stresses [33]. In particular, B toxicity causes a decrease in maize production as well as in other cereals [28,34,35]. Therefore, the search and molecular characterization of new maize varieties with improved tolerance to B toxicity has become an interesting research topic. In a recent work, two Peruvian maize landraces (Pachía and Sama) were tested for tolerance to high B. The Sama landrace had greater tolerance to B excess than Pachía [27]. In this work, a comparative proteomic characterization of these two maize landraces with different tolerance to B toxicity was performed to improve our molecular knowledge about which proteins are involved in B-toxicity tolerance.

2. Results

A total of 2793 proteins were identified in at least one of the biological replicates of a landrace (Sama or Pachía) and a B treatment analyzed (Table S1a). In addition, the number of proteins detected in both Pachía and Sama in each of the B treatments studied was similar being close to 1100 proteins (Table 1).

Table S1a shows the dataset of the identified proteins indicating their gene ontology (GO) biological processes (GOBP), GO molecular functions (GOMF), and GO cellular compartments (GOCC), and Table S1b summarizes the statistical analysis and fold changes of the proteins. To study the differentially accumulated proteins in Pachía and Sama in both B treatments, four comparison groups were established: 1) Sama and Pachía seedlings subjected to the control B condition (S0.05/P0.05), 2) Sama and Pachía treated with 10 mM B (S10/P10), 3) Sama subjected to 10 mM and 0.05 mM B (S10/S0.05), and 4) Pachía treated with 10 mM and 0.05 mM B (P10/P0.05). A total of 303 proteins had statistically significant differential expression ($P \leq 0.05$) in the above groups (Table S2). The S0.05/P0.05 and S10/P10 groups contain those proteins that were differentially expressed between Sama and Pachía in 0.05 mM or 10 mM B, respectively. In media with 0.05 mM B, more proteins were up- and down-accumulated between Sama and Pachía than in 10 mM B (Figure 1 and Table 1). In addition, the S10/S0.05 and P10/P0.05 comparison groups included proteins that were differentially expressed in response to B toxicity in Sama or Pachía, respectively. Pachía had a higher number of proteins induced and repressed by B toxicity than Sama, thus 98 proteins were up-expressed in Pachía in 10 mM B while only 38 in Sama and 51 proteins were down-expressed in Pachía under B toxicity versus 28 in Sama (Figure 1).

Table 1. Number of proteins detected in leaves of Pachía (P) and Sama (S) landraces under different boron (B) treatments and number of significant differentially accumulated proteins (DAPs) in Pachía and Sama landraces under different B treatments.

	P0.05 mM (Control)	**P10 mM B (B toxicity)**	**S0.05 mM (control)**	**S10 mM (B toxicity)**
Number of detected proteins[1]	1100	1040	1111	1145
		S0.05 versus P0.05 (Control conditions)		**S10 versus P10 (B toxicity conditions)**
Number of significant DAPs between Sama and Pachía		99		60
		Sama S10 versus S0.05		**Pachía P10 versus P0.05**
Number of significant DAPs by B toxicity		66		149

[1] Numbers of proteins that were detected in at least one landrace (Sama or Pachía) and one B treatment analyzed.

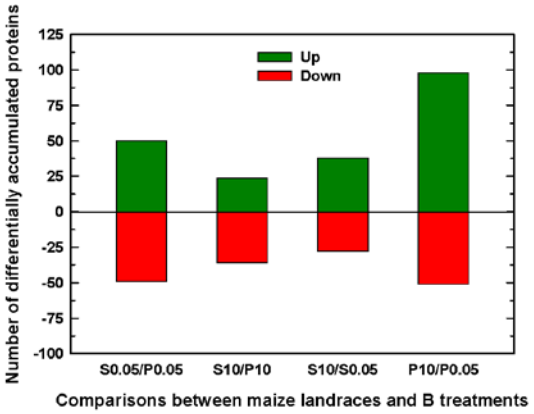

Figure 1. Number of significantly ($P \leq 0.05$) accumulated proteins up or down, represented as positive and negative, respectively, comparing maize landraces and B treatments. Seedlings were subjected to 0.05 and 10 mM B for 10 days. Results were obtained from 3-4 separate plants of each landrace and B treatments. For more details, see Materials and Methods. S: Sama landrace; P: Pachía landrace; 0.05: 0.05 mM B (B control treatment); 10: 10 mM B (B toxicity treatment). The numbers above the columns represent the numbers of proteins accumulated up (green) or down (red).

2.1. Classification into several functional categories of differentially accumulated proteins in both maize landraces and B treatments

All significant differentially expressed proteins in the four comparison groups described above were functionally classified into 26 categories using several databases (Table S2). The functional categories that included the largest number of differentially accumulated proteins were transcription and translation processes (57), photosynthesis (25), amino acid metabolism (24), protein degradation (23), carbohydrate metabolism (20), and protein stabilization and folding (18) (Figure 2 and Table S2). These main categories together contained more than 50% of the total differentially expressed proteins.

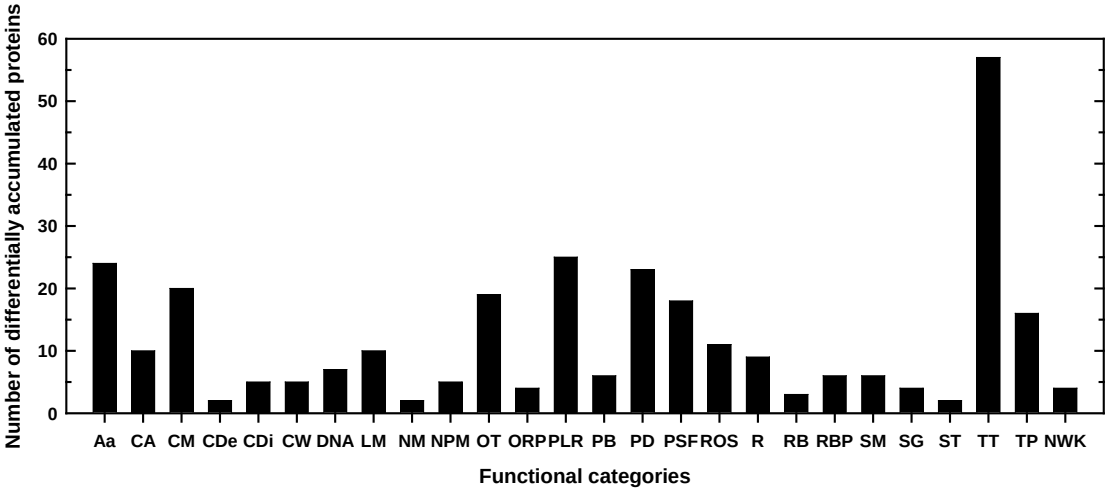

Figure 2. Number of differentially accumulated proteins (DAPs) in the different functional categories obtained from the four comparisons shown in Figure 1 and Table S2. Seedlings of Sama and Pachía landraces were subjected to 0.05 and 10 mM B for 10 days. Results were obtained by addition of the DAPs in the four comparisons. For more details, see Materials and Methods. Aa: amino acid metabolism; CA: carbon assimilation and Calvin cycle; CM: carbohydrate metabolism; CDe: cell death; CDi: cell division; CW: cell wall; DNA: DNA and chromatin organization and DNA repair; LM: lipid metabolism; NM: nitrogen metabolism; NPM: nucleotide, purine, and pyrimidine metabolism; OT: others; ORP: oxidation and reduction processes; PLR: photosynthetic light reactions; PB: pigment biosynthesis; PD: protein degradation; PSF: protein stabilization and folding; ROS: reactive oxygen species scavenging pathways/response to oxidative stress; R: respiration metabolism (glycolysis, TCA cycle, and mitochondrial electron transfer); RB: ribosome biogenesis; RBP: RNA binding and processing; SM: secondary metabolism; SG: signaling; ST: stress; TT: transcription and translation processes; TP: transporters and transport processes; NWK: not well-known proteins.

2.2. Differentially expressed proteins in Sama and Pachía in response to B toxicity

Considering that the major aim of this work was to analyze the changes provoked by B toxicity on protein expressions in Pachía and Sama, we will now focus on the proteins that were differentially expressed by B toxicity in these landraces. Thus, 66 and 149 proteins were differentially expressed in response to B toxicity in Sama and Pachía, respectively (Table 1). The main functional categories containing the highest number of differentially expressed proteins under B toxicity in both Sama and Pachía were transcription and translation, photosynthesis, amino acid metabolism, protein degradation, protein stabilization and folding, and reactive oxygen species (ROS) (Figures 3 and 4). Interestingly, most of the proteins belonging to the transcription and translation category were induced in response to B toxicity in both Sama and Pachía, the number of differentially induced proteins being remarkably higher in Pachía (Figures 3 and 4). However, almost all proteins included in the photosynthesis category were repressed in 10 mM B, the number of down-accumulated proteins being also higher in Pachía than in Sama (Figure 4 and Table S2). Regarding protein degradation, and protein stabilization and folding, most of the differentially expressed proteins in 10 mM B were found in Pachía, suggesting that B toxicity would alter the structure and folding of proteins in this landrace. In addition, many of the proteins in the ROS category were induced by B toxicity in both landraces (Figure 4 and Table S2). Although the groups of carbon assimilation and metabolism, lipid metabolism, and respiration included a smaller number of proteins that those mentioned above, nevertheless, a larger number of differentially expressed proteins were found in Pachía under B toxicity (Figure 4 and Table S2). Other interesting categories were cell death, cell division, cell wall, ribosome biogenesis, and RNA binding and processing which, despite having a very small number of proteins regulated by B toxicity, had an interesting distribution in both landraces and B treatments. In fact, in the cell death and cell wall categories, only proteins whose expressions were induced by B toxicity were found in Pachía, however, the cell division, ribosome

 doi:10.20944/preprints202305.0301.v1

biogenesis, and RNA binding and processing categories also contained proteins with higher accumulation in 10 mM B but in both landraces (Figure 4 and Table S2).

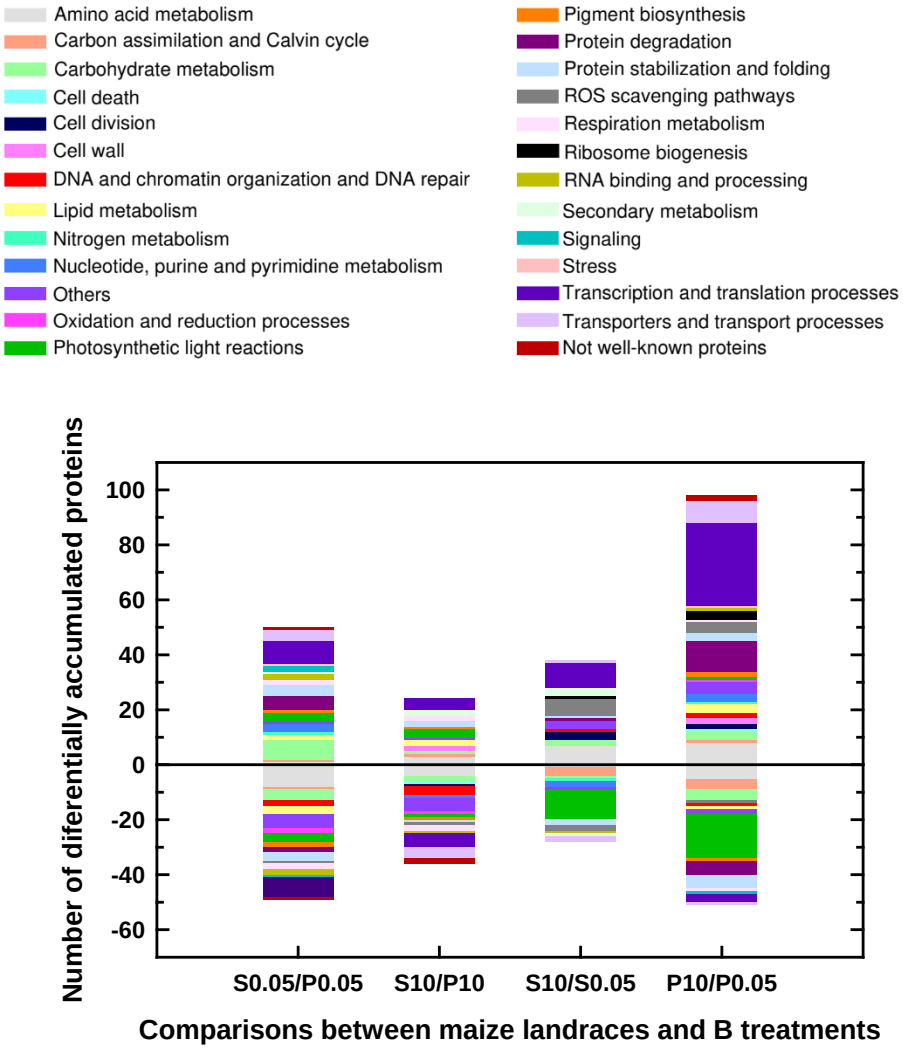

Figure 3. Functional categories of 303 maize proteins given as the number of those significantly expressed, represented as positive (up-accumulated) and negative (down-accumulated). Seedlings of Sama (S) and Pachía (P) landraces were subjected to 0.05 and 10 mM B for 10 days. Results were obtained from 3-4 separate plants of each landrace and B treatments. For more details, see Materials and Methods. 0.05: 0.05 mM B (B control treatment); 10: 10 mM B (B toxicity treatment).

A total of 18 proteins were commonly expressed (repressed or induced) in both landraces in response to B toxicity, with the amino acid metabolism and photosynthesis categories having the highest number of proteins (Table 2). All proteins of the amino acid metabolism group were up-accumulated under B toxicity conditions, with these inductions being slightly greater in Pachía than in Sama. Interestingly, however, all commonly expressed proteins from the photosynthesis category were repressed by B toxicity, these repressions being remarkably higher in Pachía than in Sama (Table 2).

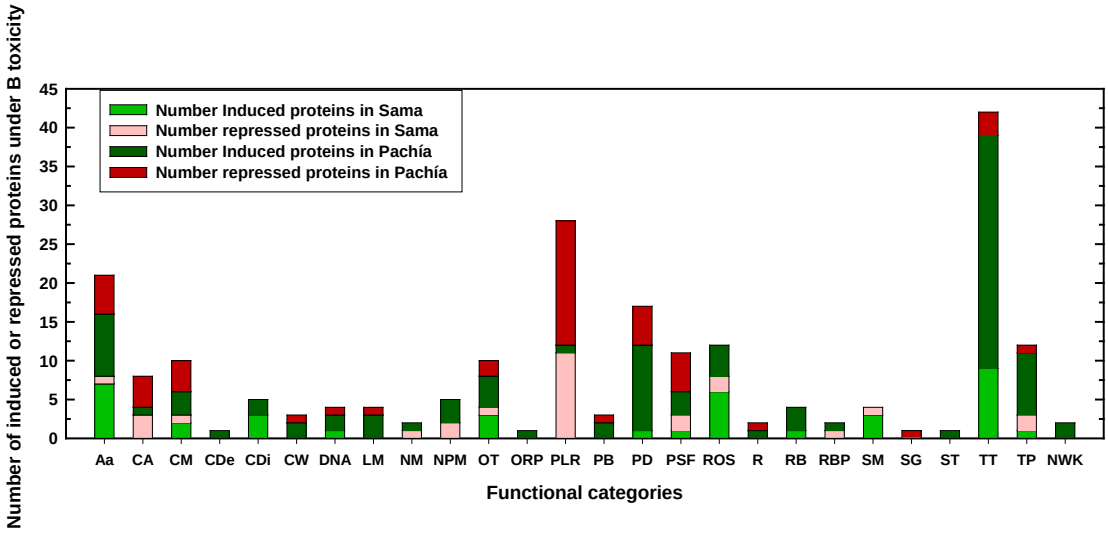

Figure 4. Number of induced or repressed proteins in Sama and Pachía landraces in the different functional categories obtained from the comparisons between B toxicity and B control conditions shown in Table S2. Seedlings of Sama and Pachía landraces were subjected to 0.05 (control) and 10 mM (toxicity) B for 10 days. Results were obtained by addition of the induced or repressed proteins in Sama and Pachía. For more details, see Materials and Methods. Aa: amino acid metabolism; CA: carbon assimilation and Calvin cycle; CM: carbohydrate metabolism; CDe: cell death; CDi: cell division; CW: cell wall; DNA: DNA and chromatin organization and DNA repair; LM: lipid metabolism; NM: nitrogen metabolism; NPM: nucleotide, purine, and pyrimidine metabolism; OT: others; ORP: oxidation and reduction processes; PLR: photosynthetic light reactions; PB: pigment biosynthesis; PD: protein degradation; PSF: protein stabilization and folding; ROS: reactive oxygen species scavenging pathways/response to oxidative stress; R: respiration metabolism (glycolysis, TCA cycle, and mitochondrial electron transfer); RB: ribosome biogenesis; RBP: RNA binding and processing; SM: secondary metabolism; SG: signaling; ST: stress; TT: transcription and translation processes; TP: transporters and transport processes; NWK: not well-known proteins.

Table 2. Commonly expressed proteins in both Pachía and Sama landraces in response to boron (B) toxicity.

			Pachía		Sama			
Protein ID[1]	**Gene Name/ID[2]**	**Protein name / Annotation**	**FC[3]**	***P*-value[4]**	**FC[3]**	***P*-value[4]**	**FCSA/ FCPA[5]**	**Function/Biological process[6]**
Amino acid metabolism								
B6SKB7	Zm00001d031013	Methylcrotonoyl-CoA carboxylase subunit α	4.44	0.0022	3.56	0.0049	0.80	Leucine degradation
A0A1D6K836	Zm00001d029848	Branched-chain-amino-acid aminotransferase	2.35	0.0272	1.65	0.0241	0.70	Branched-chain amino acid biosynthesis
B4G011	Zm00001d046923	D-3-phosphoglycerate dehydrogenase chloroplastic	2.31	0.0154	1.52	0.0202	0.66	Serine biosynthesis
A0A1D6DW07	Zm00001d002051	D-3-phosphoglycerate dehydrogenase	1.78	0.0494	1.69	0.0175	0.95	Serine biosynthesis
Carbon assimilation / Calvin cycle								
O24574	Zm00001d004894	Ribulose bisphosphate carboxylase small chain	0.38	0.0113	0.33	0.0466	0.87	Carbon dioxide fixation

Carbohydrate metabolism								
Q9FQ11	Zm00001d010523	Sucrose-phosphatase 1	1.50	0.0154	1.58	0.0420	1.05	Sucrose biosynthesis
A0A1D6IJ76	Zm00001d022107	Glyceraldehyde-3-phosphate dehydrogenase A	0.34	0.0319	0.51	0.0019	1.52	Carbon metabolism
Cell division								
A0A1D6FRI4	Zm00001d010500	ERBB-3 binding protein 1	1.89	0.0387	1.58	0.0266	0.84	Cell division and cell growth regulation
Photosynthetic light reactions								
A0A1D6HS38	Zm00001d018779	Oxygen-evolving enhancer protein 2-1 chloroplastic (OEE2-1)	0.27	0.0110	0.48	0.0354	1.78	Photosynthesis. Photosystem II oxygen evolving complex
B4FWG2	Zm00001d048422	Photosynthetic NDH subunit of subcomplex B 2 chloroplastic	0.25	0.0047	0.41	0.0200	1.62	Photosynthetic electron transport flow around photosystem I to produce ATP
A0A1X7YHG9	AtpA	ATP synthase subunit α chloroplastic (ATPα)	0.20	0.0166	0.61	0.0163	2.99	Chloroplast ATP synthesis coupled proton transport
P46617	PetA	Cytochrome f	0.18	0.0193	0.29	0.0161	1.59	Photosynthetic electron transport activity
P00827	Zm00001d006403	ATP synthase subunit β chloroplastic (ATPβ)	0.15	0.0076	0.52	0.0274	3.45	Chloroplast ATP synthesis coupled proton transport
Reactive Oxygen Species (ROS) Scavenging Pathways / Response to oxidative stress								
A0A1D6MSE3	Zm00001d040721	Dihydrolipoyl dehydrogenase	2.30	0.0273	1.80	0.0205	0.78	Cell redox homeostasis
A0A1D6JPH3	Zm00001d027769	Glutathione reductase	2.21	0.0053	1.71	0.0436	0.77	Cell redox homeostasis. Glutathione metabolic process. Cellular oxidant detoxification
Ribosome biogenesis								
K7UTH7	Zm00001d009596	GTPase ERA1 chloroplastic	2.61	0.0108	1.81	0.0126	0.69	Ribosome biogenesis. Ribosomal small subunit assembly. rRNA processing
Transcription and translation processes								
A0A1D6LIV5	Zm00001d035802	Phenylalanine--tRNA ligase beta subunit cytoplasmic	2.56	0.0314	2.23	0.0093	0.87	Translation. Phenylalanyl-tRNA aminoacylation
Transporters and transport processes								
B6SP43	Zm00001d007597	ABC family1	4.54	0.0103	2.69	0.0125	0.59	ATPase-coupled transmembrane transporter activity

[1]Proteins ID, Protein identification (ID) number in the UniProt database; [2]Gene Name, name or ID number of the corresponding gene of the differentially expressed protein as searched in the Maize Genetics and Genomics Database (MaizeGDB; https://www.maizegdb.org/; [3]Fold Change, is expressed as the ratio of LFQ intensities (on a logarithmic scale) of proteins between 10 and 0.05 mM B treatments; [4]*P*-value, statistical level (using Student's *t*-test) ≤ 0.05, at which differential protein expression was accepted as significant; [5]FCSA/FCPA, is the ratio between fold change of Sama and Pachía. [6]Function/Biological process, annotated biological functions or biological process based on different databases. Induced proteins are highlighted with light green rows and repressed proteins with light red rows. For more details, see Materials and Methods. Results were obtained from 3-4 separate plants of each landrace.

Tables 3 and 4 list the most strongly differentially expressed proteins that were up- or down-regulated more than twofold by B toxicity in Pachía and Sama, respectively. In Pachía, 105 proteins had strong differential expression under B toxicity, while only 27 were found in Sama. Photosynthesis was the functional category containing the highest number of proteins whose expressions were strongly down-accumulated in response to B toxicity in both Pachía and Sama, however, interestingly, both minor number of repressed and very strongly repressed (FC <0.33) proteins were observed in Sama (Tables 3,4, and S2). Different subunits of the NDH complex (NDHS, B1, B2, J, and H) were strongly repressed by B toxicity in Pachía but not in Sama (Tables 3, 4, and S2). In addition, only in Pachía were detected proteins related to protein degradation processes whose expressions were mainly induced by B toxicity suggesting that enhanced damage would be provoked by 10 mM B in Pachía proteins (Table 3). Furthermore, B toxicity markedly induced a larger number (15) of proteins in Pachía belonging to the transcription and translation category (Table 3).

Table 3. Proteins with higher differential expression in Pachía leaves in response to boron (B) toxicity. This table shows the proteins strongly induced or repressed by B toxicity in Pachía by comparing their expressions with those of Pachía in medium with 0.05 mM B.

Protein ID[1]	Gene Name/ID[2]	Protein name/Annotation	FC[3]	*P*-Value[4]	Function/Biological process[5]
AMINO ACID AND PEPTIDE METABOLISMS					
Strongly induced proteins by B toxicity in Pachía					
B6SKB7	Zm00001d031013	Methylcrotonoyl-CoA carboxylase subunit α	4.44	0.0022	Leucine degradation
B6SWZ4	Zm00001d050336	Methylcrotonoyl-CoA carboxylase β chain mitochondrial	2.85	0.0154	Leucine degradation
A0A1D6K836	Zm00001d029848	Branched-chain-amino-acid amino-transferase	2.35	0.0272	Branched-chain amino acid biosynthesis
B4G011	Zm00001d046923	D-3-phosphoglycerate dehydroge-nase chloroplastic	2.31	0.0154	Serine biosynthesis
C4J411	Zm00001d028464	Imidazole glycerol phosphate synthase hisHF	2.17	0.0017	Histidine biosynthesis
C4JBG7	Zm00001d015088	3-isopropylmalate dehydratase large subunit	2.14	0.0320	Leucine biosynthesis
Strongly repressed proteins by B toxicity in Pachía					
B4FUH2	Zm00001d043382	Aspartate aminotransferase	0.48	0.0195	Amino acid metabolic process
B4FU01	Zm00001d045153	Cystathionine β-lyase chloroplas-tic	0.44	0.0235	Methionine biosynthetic. Cysteine biosynthetic process via cystathionine
A0A1D6ICL3	Zm00001d021596	Adenosine 5-phosphosulfate reductase-like1	0.29	0.0140	Cysteine biosynthetic process. Sulfate reduction
B6TZD1	Zm00001eb168430	Methylthioribose-1-phosphate isomerase	0.24	0.0461	Methionine biosynthesis

CARBON ASSIMILATION AND CALVIN CYCLE					
Strongly induced proteins by B toxicity in Pachía					
A0A1D6FQE4	Zm00001d010321	Pyruvate phosphate dikinase	2.31	0.0449	C4 photosynthetic carbon assimilation cycle
Strongly repressed proteins by B toxicity in Pachía					
O24574	Zm00001d004894	Ribulose bisphosphate carboxylase small chain	0.38	0.0113	Carbon dioxide fixation
B4FQ59	Zm00001d017711	Phosphoribulokinase	0.33	0.0004	Calvin- Benson cycle
Q9ZT00	Zm00001eb164390	Ribulose bisphosphate carboxylase/oxygenase activase chloroplastic	0.26	0.0090	Carbon dioxide fixation. Rubisco activator activity
CARBOHYDRATE METABOLISM					
Strongly induced proteins by B toxicity in Pachía					
A0A1D6NE29	Zm00001d043662	α-amylase 3 chloroplastic	2.05	0.0460	Starch degradation
Strongly repressed proteins by B toxicity in Pachía					
A0A1D6M7C2	Zm00001d038579	Phosphoglycerate kinase cytosolic	0.49	0.0136	Glycolysis and gluconeogenesis
B4FRC9	Zm00001d011965	Transaldolase	0.41	0.0407	Pentose-phosphate shunt
A0A1D6IJ76	Zm00001d022107	Glyceraldehyde-3-phosphate dehydrogenase A	0.34	0.0319	Carbon metabolism
CELL DEATH					
Strongly induced proteins by B toxicity in Pachía					
B4F8B9	Zm00001d018468	S-(hydroxymethyl)glutathione dehydrogenase	2.81	0.0027	Cell death. Formaldehyde oxidation (glutathione-dependent)
CELL WALL					
Strongly induced proteins by B toxicity in Pachía					
B4F9J1	Zm00001d046357	β-galactosidase	3.17	0.0092	Xyloglucan degradation
DNA AND CHROMATIN ORGANIZATION AND DNA REPAIR					
Strongly induced proteins by B toxicity in Pachía					
B6TGH8	Zm00001d034479	Histone H1	3.60	0.0349	Chromosome condensation. Nucleosome assembly. Nucleosome positioning
C0P6Q6	Zm00001d040416	DNA gyrase subunit B	3.48	0.0007	DNA topological change
Strongly repressed proteins by B toxicity in Pachía					
B6SK03	Zm00001d053295	Ubiquitin-conjugating enzyme E2 variant 1C	0.39	0.0409	DNA postreplication repair. Protein polyubiquitination
LIPID METABOLISM					
Strongly induced proteins by B toxicity in Pachía					
K7VQG5	Zm00001d008727	Phospholipase D	2.30	0.0244	Phospholipid degradation
A0A1D6NE81	Zm00001d043680	Phospholipase A1-IIδ	2.02	0.0390	Lipid degradation
Strongly repressed proteins by B toxicity					
B4FLS8	Zm00001d003584	12-oxo-phytodienoic acid reductase 5	0.33	0.0436	Fatty acid and oxylipin biosynthesis
NITROGEN METABOLISM					
Strongly induced proteins by B toxicity in Pachía					

A0A1D6PZA5	Zm00001d049995	Nitrate reductase	2.19	0.0077	Nitrate reductase (NADH) activity. Nitrate assimilation
OTHERS					
Strongly induced proteins by B toxicity in Pachía					
A0A1D6JGY3	Zm00001d026515	Molybdopterin molybdenum-transferase	2.92	0.0023	Molybdenum cofactor biosynthesis
A0A1D6HUN3	Zm00001d019040	D-2-hydroxyglutarate dehydrogenase mitochondrial	2.09	0.0380	Lysine degradation
Strongly repressed proteins by B toxicity in Pachía					
C0PDB6	Zm00001d039535	HXXXD-type acyl-transferase family protein	0.40	0.0112	N-acyltransferase activity
C0PE12	Zm00001d009877	Protein plastid transcriptionally active 16 chloroplastic	0.24	0.0121	Circadian rhythm
OXIDATION AND REDUCTION PROCESSES					
Strongly induced proteins by B toxicity in Pachía					
A0A1D6M498	Zm00001d038189	FAD/NAD(P)-binding oxidoreductase family protein	2.04	0.0101	Oxidoreductase activity
PHOTOSYNTHETIC LIGHT REACTIONS					
Strongly repressed proteins by B toxicity in Pachía					
B6SSB9	Zm00001d035859	Plastocyanin	0.50	0.0300	Photosynthetic electron transport
A0A1D6GU53	Zm00001d014564	Oxygen-evolving enhancer protein 1-1 chloroplastic	0.47	0.0268	Photosynthesis. Oxygen evolving activity. Photosystem II assembly and stabilization
B6SUC4	Zm00001d046786	Chlorophyll a-b binding protein, chloroplastic	0.41	0.0086	Photosynthesis. Light harvesting in photosystem I
B6T927	Zm00001d014349	NAD(P)H-quinone oxidoreductase subunit S chloroplastic (NDHS)	0.39	0.0095	Photosynthetic electron transport chain
P25709	NdhH	NAD(P)H-quinone oxidoreductase subunit H, chloroplastic	0.37	0.0022	Photosynthesis, light reaction. Photosynthetic electron transport chain. Couples the photosynthetic redox reaction to proton translocation
B6SP99	Zm00001d024148	Photosynthetic NDH subunit of subcomplex B 1 chloroplastic	0.33	0.0137	Photosynthetic electron transport in photosystem I
B4FJP7	Zm00001d027729	Photosynthetic NDH subunit of subcomplex B 2 chloroplastic	0.32	0.0169	Photosynthetic electron transport in photosystem I
B4FR80	Zm00001d033098	Post-illumination chlorophyll fluorescence increase (ZmPIFI)	0.28	0.0270	Chlororespiration
A0A1D6HS38	Zm00001d018779	Oxygen-evolving enhancer protein 2-1 chloroplastic (OEE2-1)	0.27	0.0110	Photosynthesis. Photosystem II oxygen evolving complex

B4FWG2	Zm00001d048422	Photosynthetic NDH subunit of subcomplex B 2 chloroplastic	0.25	0.0047	Photosynthetic electron transport flow around photosystem I to produce ATP
P19124	NdhJ	NAD(P)H-quinone oxidoreductase subunit J, chloroplastic	0.22	0.0147	Photosynthesis, light reaction, photosynthetic electron transport chain. Couples the photosynthetic redox reaction to proton translocation
A0A1X7YHG9	AtpA	ATP synthase subunit α (ATPα)	0.20	0.0166	Chloroplast ATP synthesis coupled proton transport
P46617	PetA	Cytochrome f	0.18	0.0193	Photosynthetic electron transport chain
P00827	Zm00001d009488	ATP synthase subunit β, chloroplastic (ATPβ)	0.15	0.0076	Chloroplast ATP synthesis coupled proton transport
A0A1D6JYG6	Zm00001d028670	Photosynthetic NDH subunit of lumenal location 1 chloroplastic	0.13	0.0134	Part of photosystem II oxygen evolving complex
PIGMENT BIOSYNTHESIS					
Strongly repressed proteins by B toxicity in Pachía					
A0A1D6FAV8	Zm00001d008203	Protoporphyrinogen oxidase	0.38	0.0173	3,8-divinyl-chlorophyllide a and protoporphyrinogen IX biosynthesis
PROTEIN DEGRADATION					
Strongly induced proteins by B toxicity in Pachía					
B4FS65	Zm00001d005391	Cysteine protease 14	4.38	0.0146	Proteolysis. Proteolysis involved in protein catabolic process
A0A1D6HM49	Zm00001d018282	Subtilisin-like protease SBT1.4	3.70	0.0399	Serine protease. Serine-type endopeptidase activity. Proteolysis
A0A1D6H4R4	Zm00001d015962	Prolyl oligopeptidase family protein	3.58	0.0080	Proteolysis. Serine protease. Serine-type peptidase activity
Q84TL7	Zm00001d011036	Legumin-like protein	2.86	0.0453	Protein ubiquitination. Nutrient reservoir activity. Storage protein
A0A1D6KWW2	Zm00001d033194	Subtilisin-like protease	2.85	0.0403	Proteolysis. Serine protease. Serine-type endopeptidase activity
A0A1D6KV27	Zm00001d032956	Acylamino-acid-releasing enzyme	2.54	0.0086	Proteolysis. Serine protease. Serine-type endopeptidase activity
C0HI51	Zm00001d044102	Zn-dependent exopeptidase superfamily protein	2.53	0.0131	Proteolysis. Aminopeptidase. Metalloaminopeptidase activity
Q84TL6	Zm00001d035597	Legumin-like protein	2.36	0.0386	Protein ubiquitination. Storage protein. Nutrient reservoir activity

A0A1D6HL34	Zm00001d018145	Presequence protease 2 chloroplastic/mitochondrial	2.22	0.0180	Proteolysis. Metalloendopeptidase activity. Protein processing
K7VGG8	Zm00001d010522	ATP-dependent zinc metalloprotease FTSH 10 mitochondrial	2.07	0.0359	Proteolysis. Metalloprotease mitochondrial
C4JC43	Zm00001d049100	Target of Myb protein 1	2.04	0.0450	Proteolysis. Protein transport to vacuole involved in ubiquitin-dependent protein catabolic process via the multivesicular body sorting pathway
Strongly repressed proteins by B toxicity in Pachía					
A0A1D6H558	Zm00001d016036	Chloroplast processing peptidase	0.47	0.0438	Protease. Serine-type endopeptidase activity
B4FQJ6	Zm00001d018309	26S protease regulatory subunit 7 homolog A	0.46	0.0249	Proteolysis. Protein catabolic process. Peptidase activity
A0A1D6FKP2	Zm00001d009613	Protease Do-like 1 chloroplastic	0.45	0.0496	Proteolysis. Serine-type endopeptidase activity
K7TTX0	Zm00001d025628	Plant UBX domain-containing protein 4	0.44	0.0107	Proteasome-mediated ubiquitin-dependent protein catabolic process
PROTEIN STABILIZATION AND FOLDING					
Strongly induced proteins by B toxicity in Pachía					
A0A1D6FN98	Zm00001d009948	Heat shock 70 kDa protein 14	2.28	0.0487	Protein folding. Stress response
B6SZ69	Zm00001d028630	Heat shock cognate 70 kDa protein 2	2.02	0.0398	Protein refolding. Stress response
Strongly repressed proteins by B toxicity in Pachía					
A0A1D6KC46	Zm00001d030346	Hsp20/alpha crystallin family protein	0.49	0.0499	Chaperone. Response to heat
C0PKD9	Zm00001d052101	Chaperonin10	0.42	0.0428	Chaperone cofactor-dependent protein refolding
G2XK63	Zm00001d040257	T-complex protein 1 subunit beta	0.27	0.0065	Protein folding. Chaperone
B4FR04	Zm00001d019052	Peptidylprolyl isomerase	0.23	0.0205	Protein folding. Rotamase
REACTIVE OXYGEN SPECIES (ROS) SCAVENGING PATHWAYS / RESPONSE TO OXIDATIVE STRESS					
Strongly induced proteins by B toxicity in Pachía					
A0A1D6K5D2	Zm00001d029457	Nucleoredoxin1	2.91	0.0117	Protection against oxidative stress. Cellular oxidant detoxification
A0A1D6MSE3	Zm00001d040721	Dihydrolipoyl dehydrogenase	2.30	0.0273	Cell redox homeostasis
A0A1D6JPH3	Zm00001d027769	Glutathione reductase	2.21	0.0053	Cell redox homeostasis. Cellular oxidant detoxification.

					Glutathione metabolic process.
K7US39	Zm00001d009163	Dihydrolipoyl dehydrogenase	2.19	0.0088	Cell redox homeostasis
RIBOSOME BIOGENESIS					
Strongly induced proteins by B toxicity in Pachía					
B4FPB7	Zm00001d006100	60S ribosomal protein L7a	2.63	0.0051	Ribosome biogenesis. Maturation of LSU-rRNA
K7UTH7	Zm00001d009596	GTPase ERA1 chloroplastic	2.61	0.0108	Ribosome biogenesis. Ribosomal small subunit assembly. rRNA processing
B4F7Y1	Zm00001d031640	60S ribosomal protein L7a-1	2.39	0.0448	Ribosomal protein. Maturation of LSU-rRNA
RNA BINDING AND PROCESSING					
Strongly induced proteins by B toxicity in Pachía					
A0A1D6HT50	Zm00001d018891	Chloroplast RNA processing 4	2.60	0.0142	mRNA catabolic process
SIGNALING					
Strongly repressed proteins by B toxicity in Pachía					
P49235	Zm00001eb411380	4-hydroxy-7-methoxy-3-oxo-3,4-dihydro-2H-1,4-benzoxazin-2-yl glucoside beta-D-glucosidase 1, chloroplastic	0.19	0.0090	Cytokinin signaling pathway
STRESS					
Strongly induced proteins by B toxicity in Pachía					
B4F9K2	Zm00001d005315	Calcium-dependent lipid-binding (CaLB domain) family protein	2.11	0.0402	Defense response. Response to stress
TRANSCRIPTION AND TRANSLATION PROCESSES					
Strongly induced proteins by B toxicity in Pachía					
A0A1D6LEN8	Zm00001d035139	MA3 domain-containing protein	4.95	0.0073	Negative regulation of transcription, DNA-templated. Regulation of translation
Q6R9D1	GRMZM5G806488	Ribosomal protein S7	3.89	0.0202	Translation. Ribosomal small subunit assembly. Structural constituent of ribosome
A0A1D6IAN8	Zm00001d021400	Octicosapeptide/Phox/Bem1p (PB1) domain-containing protein / tetratricopeptide repeat (TPR)-containing protein	3.47	0.0323	RNA processing
C0P456	Zm00001d002789	Pentatricopeptide repeat-containing protein	3.26	0.0259	Likely involved in posttranscriptional control of gene expression in organelles
A0A1D6NR59	Zm00001d044745	Probable alanine--tRNA ligase, chloroplastic	2.74	0.0097	Translation. Alanyl-tRNA aminoacylation
A0A1D6LIV5	Zm00001d035802	Phenylalanine--tRNA ligase beta subunit cytoplasmic	2.56	0.0314	Translation. Phenylalanyl-tRNA aminoacylation

B6T5F2	Zm00001d011992	60S ribosomal protein L13	2.48	0.0387	Translation. Structural constituent of ribosome
A0A1D6HM03	Zm00001d018274	Isoleucine--tRNA ligase chloroplastic/mitochondrial	2.29	0.0087	Translation. Isoleucyl-tRNA aminoacylation
A0A1D6QAN9	Zm00001d051885	ATG8-interacting protein 1	2.28	0.0047	Box C/D RNA 3'-end processing. rRNA processing
A0A1D6FRP3	Zm00001d010530	Cysteine--tRNA ligase 1 cytoplasmic	2.26	0.0470	Translation. Cysteinyl-tRNA aminoacylation
B4FMD3	Zm00001d012978	40S ribosomal protein S23-2	2.13	0.0451	Translation. Structural constituent of ribosome
K7UTZ2	Zm00001d009761	Spliceosome RNA helicase BAT1 isoform 1	2.10	0.0455	RNA splicing. RNA helicase activity
K7TY03	Zm00001d023741	Alanine--tRNA ligase	2.07	0.0144	Translation. Alanyl-tRNA aminoacylation
B4FYR2	Zm00001d038865	60S ribosomal protein L28	2.05	0.0275	Translation. Structural constituent of ribosome
B6U151	Zm00001d002104	Glutamyl-tRNA(Gln) amidotransferase subunit A, chloroplastic/mitochondrial	2.02	0.0464	Mitochondrial translation
Strongly repressed proteins by B toxicity in Pachía					
C0P7X7	Zm00001d034808	30S ribosomal protein S6 alpha chloroplastic	0.50	0.0059	Translation. Structural constituent of ribosome
B4FUZ5	Zm00001d047581	30S ribosomal protein S1	0.46	0.0055	Translation. Ribosomal protein
O50018	Zm00001d046449	Elongation factor 1-α	0.29	0.0269	Translation. Translation elongation factor activity
TRANSPORTERS AND TRANSPORT PROCESSES					
Strongly induced proteins by B toxicity in Pachía					
B6SP43	Zm00001d007597	ABC family1	4.54	0.0103	ATPase-coupled transmembrane transporter activity
A0A1D6H2R4	Zm00001d015569	H^+-exporting diphosphatase	4.34	0.0050	Ion transport. Pyrophosphate hydrolysis-driven proton transmembrane transporter activity
A0A1D6MS70	Zm00001d040686	Protein translocase subunit SECA1 chloroplastic	4.12	0.0173	Protein transport
A0A1D6DSW6	Zm00001d001788	K^+ efflux antiporter 2 chloroplastic	3.79	0.0414	Chloroplast potassium ion trans-port
B6T5R1	Zm00001d010504	Ran-binding protein 1	3.16	0.0492	Intracellular transport. Protein and mRNA transport. Nucleocytoplasmic transport
A0A1D6KSB0	Zm00001d032615	Protein TIC110 chloroplastic	2.35	0.0118	Protein import into chloroplast stroma
NOT WELL-KNOWN PROTEINS					
Strongly induced proteins by B toxicity in Pachía					
A0A1D6KKK1	Zm00001d031677	MtN19-like protein	2.62	0.0464	Not well determined
A0A1D6JI62	Zm00001d026632	Stem-specific protein TSJT1	2.43	0.0283	Not well determined

Only proteins considered differentially expressed, namely those with fold-changes ≥2.0 or ≤ 0.5 and *P*-values ≤ 0.05, are shown in this table. Induced proteins are highlighted with light green rows and repressed proteins with light red rows. [1]Proteins ID, Protein identification number in the UniProt database. [2]Gene Name, name or ID number of the corresponding gene of the differentially expressed protein as searched in the Maize Genetics and Genomics Database (MaizeGDB; https://www.maizegdb.org/). [3]Fold Change, is expressed as the ratio of LFQ intensities (on a logarithmic scale) of proteins between 10 and 0.05 mM B treatments in Pachía. Results were obtained from 3-4 separate plants. [4]*P*-value, statistical level (using Student's *t*-test) below ≤0.05, at which differential protein expression was accepted as significant. [5]Function/Biological process, annotated biological functions or biological process based on different databases. For more details, see Materials and Methods.

Table 4. Proteins with higher differential expression in Sama leaves in response to boron (B) toxicity. This table shows the proteins strongly induced or repressed by B toxicity in Sama by comparing their expressions with those of Sama in medium with 0.05 mM B.

Protein ID[1]	Gene Name/ID[2]	Protein name/Annotation	FC[3]	*P*-value[4]	Function/Biological process[5]
AMINO ACID AND PEPTIDE METABOLISMS					
Strongly induced proteins by B toxicity in Sama					
B6SKB7	Zm00001d031013	Methylcrotonoyl-CoA carboxylase subunit alpha	3.56	0.0049	Leucine degradation
C4J3S6	Zm00001d004960	2-isopropylmalate synthase 1 chloroplastic	2.17	0.0025	Leucine biosynthesis
CARBON ASSIMILATION AND CALVIN CYCLE					
Strongly repressed proteins by B toxicity in Sama					
O24574	Zm00001d004894	Ribulose bisphosphate carboxylase small chain	0.33	0.0466	Carbon dioxide fixation
P05348	Rbcs	Ribulose bisphosphate carboxylase small chain, chloroplastic	0.13	0.0096	Carbon dioxide fixation
CELL DIVISION					
Strongly induced proteins by B toxicity in Sama					
C0P4T2	Zm00001d042664	Patellin-1	3.05	0.0149	Cell division and cell cycle
NUCLEOTIDE, PURINE AND PYRIMIDINE METABOLISM					
Strongly repressed proteins by B toxicity in Sama					
A0A1D6P7V2	Zm00001d047217	5-hydroxyisourate hydrolase	0.50	0.0136	Purine metabolism
PHOTOSYNTHETIC LIGHT REACTIONS					
Strongly repressed proteins by B toxicity in Sama					
A0A1D6HS38	Zm00001d018779	Oxygen-evolving enhancer protein 2-1 chloroplastic (OEE2-1)	0.48	0.0354	Photosynthesis. Photosystem II oxygen evolving complex
B6SSN3	Zm00001d015385	Chlorophyll a-b binding protein, chloroplastic	0.43	0.0435	Light harvesting in photosystem I
B4FWG2	Zm00001d048422	Photosynthetic NDH subunit of subcomplex B 2 chloroplastic	0.41	0.0200	Photosynthetic electron transport flow around photosystem I to produce ATP
P06670	NdhK	NAD(P)H-quinone oxidoreductase subunit K, chloroplastic	0.38	0.0149	Photosynthetic electron transport coupled photosynthetic proton transport
A0A1X7YHF7	PsbD	Photosystem II D2 protein	0.35	0.0347	Photosynthetic electron transport in photosystem II

P46617	PetA	Cytochrome f	0.29	0.0161	Photosynthetic electron transport chain
B6SQV5	Zm00001d049387	Photosystem II 10 kDa polypeptide	0.14	0.0438	Photosynthesis. Photosystem II oxygen evolving complex
PROTEIN STABILIZATION AND FOLDING					
Strongly repressed proteins by B toxicity in Sama					
A0A1D6GJM6	Zm00001d013455	Peptidylprolyl isomerase	0.40	0.0275	Protein folding. Rotamase
C4J6Y2	Zm00001d018077	Peptidylprolyl isomerase	0.18	0.0422	Protein folding. Rotamase
REACTIVE OXYGEN SPECIES (ROS) SCAVENGING PATHWAYS / RESPONSE TO OXIDATIVE STRESS					
Strongly induced proteins by B toxicity in Sama					
B4FSM5	Zm00001d040341	Peroxiredoxin	2.68	0.0112	Cellular response to oxidative stress. Hydrogen peroxide catabolic process. Cell redox homeostasis
Strongly repressed proteins by B toxicity in Sama					
B6U038	Zm00001d005482	Thiol-disulfide isomerase and thioredoxins	0.44	0.0223	Antioxidant activity. Cellular oxidant detoxification. Thioredoxin-dependent peroxiredoxin activity
B4FZ35	Zm00001d002240	CHL-*Zea mays* chloroplastic li-pocalin	0.31	0.0272	Response to oxidative stress. Violaxanthin, antheraxanthin and zeaxanthin interconversion
SECONDARY METABOLISM					
Strongly induced proteins by B toxicity in Sama					
O64411	Zm00001d024281	Polyamine oxidase 1 (PAO1)	3.34	0.0108	Spermine degradation. Amine and polyamine degradation
Strongly repressed proteins by B toxicity in Sama					
B6TAE7	Zm00001d028575	Tropinone reductase	0.44	0.0313	Tropane alkaloid biosynthesis
STRESS					
Strongly induced proteins by B toxicity in Sama					
A0A1D6NJS4	Zm00001d044222	Tetratricopeptide repeat (TPR)-containing protein	2.12	0.0428	N-terminal peptidyl-methionine acetylation. Protein maturation
TRANSCRIPTION AND TRANSLATION PROCESSES					
Strongly induced proteins by B toxicity in Sama					
A0A1D6IBP5	Zm00001d021507	Asparagine--tRNA ligase chloroplastic/mitochondrial	2.66	0.0491	Translation. Asparaginyl-tRNA aminoacylation
B4FSE0	Zm00001d033913	Alba DNA/RNA-binding protein	2.48	0.0244	Translational initiation. RNA binding
B6T872	Zm00001d021020	60S ribosomal protein L32	2.28	0.0415	Translation. Structural constituent of ribosome
A0A1D6LIV5	Zm00001d035802	Phenylalanine--tRNA ligase beta subunit cytoplasmic	2.23	0.0093	Translation. Phenylalanyl-tRNA aminoacylation
B4FJ27	Zm00001d011741	40S ribosomal protein S24	2.13	0.0363	Translation. Structural constituent of ribosome
TRANSPORTERS AND TRANSPORT PROCESSES					
Strongly induced proteins by B toxicity in Sama					
B6SP43	Zm00001d007597	ABC family1	2.69	0.0125	ATPase-coupled transmembrane transporter activity

Only proteins considered differentially expressed namely those with fold-changes ≥2.0 or ≤ 0.5 and *P*-values ≤ 0.05, are shown in this table. Induced proteins are highlighted with light green rows and repressed proteins with light red rows. [1]Proteins ID, Protein identification number in the UniProt database. [2]Gene Name, name or ID number of the corresponding gene of the differentially expressed protein as searched in the Maize Genetics and Genomics Database (MaizeGDB; https://www.maizegdb.org/). [3]Fold Change, is expressed as the ratio of LFQ intensities (on a logarithmic scale) of proteins between 10 and 0.05 mM B treatments in Sama. Results were obtained from 3-4 separate plants. [4]*P*-value, statistical level (using Student's *t*-test), at which differential protein expression was accepted as significant (≤0.05). [5]Function/Biological process, annotated biological functions or biological process based on different databases. For more details, see Materials and Methods.

Table 5 shows the proteins that were strongly up- or down-accumulated when protein expressions of Sama were compared to those of Pachía in media with 10 mM B. Sama had a remarkable up-accumulation of four proteins involved in photosynthesis (ZmPIFI and OEE2-1), chlorophyll biosynthesis (ChlH1), and secondary metabolism (PAO1) being, in addition, this last protein strongly induced in response to B toxicity (Tables 4 and 5). However, in Pachía several proteins were detected with a strong accumulation in 10 mM B when compared with Sama (shown in Table 5 as strongly down-accumulated proteins in Sama) highlighting, among them, histone H1 and ribosomal protein S7 which, besides, were strongly induced by B toxicity (Tables 3 and 5).

Table 5. Proteins with higher differential expression between Sama and Pachía leaves under boron (B) toxicity condition. This table shows the strongly up- or down-accumulated proteins in Sama in media with 10 mM B compared to those of Pachía in 10 mM B.

Protein ID[1]	Gene Name/ID[2]	Protein name/Annotation	FC[3]	*P*-value[4]	Function/Biological process[5]
AMINO ACID AND PEPTIDE METABOLISMS					
Strongly up-accumulated proteins in Sama in media with 10 mM B					
A0A1D6ICL3	Zm00001d021596	Adenosine 5-phosphosulfate reductase-like1	2.33	0.0417	Cysteine biosynthetic process. Sulfate reduction
CARBON ASSIMILATION AND CALVIN CYCLE					
Strongly up-accumulated proteins in Sama in media with 10 mM B					
A0A1D6EXF1	Zm00001d006520	PDK regulatory protein1	2.16	0.0167	Regulation of C4 photosynthetic carbon assimilation cycle
CARBOHYDRATE METABOLISM					
Strongly up-accumulated proteins in Sama in media with 10 mM B					
Q9SYS1	Zm00001d021702	β-amylase	2.63	0.0499	β-amylase activity. Starch degradation
Strongly down-accumulated proteins in Sama in media with 10 mM B					
A0A1D6K5L6	Zm00001d029502	Glucose-6-phosphate 1-dehydrogenase	0.36	0.0411	Pentose phosphate pathway
A0A1D6LY56	Zm00001d037480	Alkaline α galactosidase 2	0.33	0.0438	Carbohydrate metabolic process
CELL DEATH					
Strongly down-accumulated proteins in Sama in media with 10 mM B					
A0A1D6JNJ8	Zm00001d027656	Lethal leaf-spot 1	0.32	0.0016	Cell death. Chlorophyll catabolic process
CELL DIVISION					
Strongly down-accumulated proteins in Sama in media with 10 mM B					
A0A1D6JH24	Zm00001d026532	Protein RCC2	0.42	0.0214	Cell division

CELL WALL					
Strongly up-accumulated proteins in Sama in media with 10 mM B					
A0A1D6MWZ7	Zm00001d041578	Glossy6	3.27	0.043	Epicuticular wax accumulation. Intracellular trafficking of cuticular waxes
DNA AND CHROMATIN ORGANIZATION AND DNA REPAIR					
Strongly down-accumulated proteins in Sama in media with 10 mM B					
B4FQA5	Zm00001d018981	Histone1a	0.35	0.0318	Chromosome condensation. Nucleosome assembly
B6TGH8	Zm00001d034479	Histone H1	0.31	0.0138	Chromosome condensation. Nucleosome assembly. Nucleosome positioning
LIPID METABOLISM					
Strongly up-accumulated proteins in Sama in media with 10 mM B					
Q8W0V2	Zm00001d033623	Lipoxygenase 3	5.06	0.0455	Fatty acid and oxylipin biosynthesis
Q06XS3	Zm00001d053675	Lipoxygenase 10	3.44	0.0247	Fatty acid and oxylipin biosynthesis
OTHERS					
Strongly down-accumulated proteins in Sama in media with 10 mM B					
B6TY16	Zm00001d040331	SUN domain protein2	0.41	0.0262	Nuclear envelope organization
B4F7V3	Zm00001d021582	Protein phosphatase 2C isoform ε	0.39	0.0214	Protein dephosphorylation
A0A1D6HUN3	Zm00001d019040	D-2-hydroxyglutarate dehydrogenase mitochondrial	0.33	0.0024	Photorespiration
OXIDATION AND REDUCTION PROCESSES					
Strongly down-accumulated proteins in Sama in media with 10 mM B					
B4F987	Zm00001d020984	Putative sarcosine oxidase	0.23	0.0321	Sarcosine oxidase activity
PHOTOSYNTHETIC LIGHT REACTIONS					
Strongly up-accumulated proteins in Sama in media with 10 mM B					
B4FR80	Zm00001d033098	Post-illumination chlorophyll fluorescence increase (ZmPIFI)	2.52	0.0097	Chlororespiration
A0A1D6HS38	Zm00001d018779	Oxygen-evolving enhancer protein 2-1 chloroplastic (OEE2-1)	2.31	0.0325	Photosynthesis. Photosystem II oxygen evolving complex
PIGMENT BIOSYNTHESIS					
Strongly up-accumulated proteins in Sama in media with 10 mM B					
A0A1D6JHX0	Zm00001d026603	Magnesium-chelatase subunit ChlH1 chloroplastic (ChlH1)	2.90	0.0484	Chlorophyll biosynthetic process
PROTEIN STABILIZATION AND FOLDING					
Strongly down-accumulated proteins in Sama in media with 10 mM B					
A0A1D6KE29	Zm00001d030725	Heat shock protein 70	0.43	0.0406	Protein refolding. Protein folding chaperone. Cellular response to unfolded protein
RESPIRATION (GLYCOLISIS, TCA CYCLE AND MITOCHONDRIAL ELECTRON TRANSFER)					
Strongly up-accumulated proteins in Sama in media with 10 mM B					

B4G1C9	Zm00001d023606	Dihydrolipoamide acetyltransferase component of pyruvate dehydrogenase complex	2.04	0.0332	Acetyl-CoA biosynthetic process from pyruvate
Strongly down-accumulated proteins in Sama in media with 10 mM B					
A0A1D6MAK9	Zm00001d038792	Phosphotransferase	0.49	0.0331	Glycolysis
SECONDARY METABOLISM					
Strongly up-accumulated proteins in Sama in media with 10 mM B					
O64411	Zm00001d024281	Polyamine oxidase 1 (PAO1)	5.15	0.0007	Spermine degradation. Amine and polyamine degradation
TRANSCRIPTION AND TRANSLATION					
Strongly up-accumulated proteins in Sama in media with 10 mM B					
B4FP25	Zm00001d047296	40S ribosomal protein S19	6.38	0.0289	Translation. Structural constituent of ribosome. Ribosomal small subunit assembly
B6TDF7	Zm00001d019898	Plastid-specific 30S ribosomal protein 2	2.31	0.0243	Ribosomal protein. Ribonucleoprotein complex. RNA-binding
C0PEC4	Zm00001d032420	30S ribosomal protein S5 chloroplastic	2.12	0.0487	Translation. Structural constituent of ribosome
Strongly down-accumulated proteins in Sama in media with 10 mM B					
B6SX73	Zm00001d016549	60S ribosomal protein L35	0.42	0.0284	Translation. Structural constituent of ribosome
Q6R9D1	GRMZM5G806488	Ribosomal protein S7	0.35	0.0426	Translation. Structural constituent of ribosome. Ribosomal small subunit assembly
Transporter and transport processes					
Strongly down-accumulated proteins in Sama in media with 10 mM B					
A0A1D6H2R4	Zm00001d015569	H^+-exporting diphosphatase	0.33	0.0169	Ion transport. Pyrophosphate hydrolysis-driven proton transmembrane transporter activity
A0A1D6K7N5	Zm00001d029762	Hexose transporter	0.20	0.0439	Hexose transporter
Unknown or not well determined					
Strongly down-accumulated proteins in Sama in media with 10 mM B					
A0A1D6KKK1	Zm00001d031677	MtN19-like protein	0.23	0.0121	Not well determined

Only proteins considered differentially expressed namely those with fold-changes ≥2.0 or ≤ 0.5 and P-values ≤ 0.05, are shown in this table. Induced proteins are highlighted with light green rows and repressed proteins with light red rows. [1]Proteins ID, Protein identifying number in the UniProt database. [2]Gene Name, name or ID number of the corresponding gene of the differentially expressed protein as searched in the Maize Genetics and Genomics Database (MaizeGDB; https://www.maizegdb.org/). [3]Fold Change, is expressed as the ratio of LFQ intensities (on a logarithmic scale) of proteins between Sama and Pachía in media with 10 mM B. Results were obtained from 3-4 separate plants. [4]*P*-value, statistical level (using Student's *t*-test) below ≤0.05, at which protein differential expression was accepted as significant. [5]Function/Biological process, annotated biological functions or biological process based on different databases. For more details, see Materials and Methods.

Finally, in both Pachía and Sama, proteins exclusively detected in one of these landraces were found, among them, Nfc103a and eIF3a, which were only identified in Pachía in 10 mM B (Table 6).

Table 6. Proteins exclusively detected in Pachía or Sama leaves in at least one B treatment.

Protein ID[1]	Gene Name/ID[2]	Protein name/Annotation	Function/Biological process[3]
DNA AND CHROMATIN ORGANIZATION AND DNA REPAIR			
Protein exclusively detected in Pachía in 10 mM B			
A0A1D6KX75	Zm00001d033247	Nfc103a - nucleosome/chromatin assembly factor C	Nucleosome/chromatin assembly. DNA repair. Chromatin remodeling, regulation of DNA-templated transcription
OTHERS			
Protein exclusively detected in Sama in both B treatments			
K7VAT7	Zm00001d046569	Protein kinase superfamily protein with octicosapeptide/Phox/Bem1p domain	Protein serine/threonine kinase activity. Protein phosphorylation
REACTIVE OXYGEN SPECIES (ROS) SCAVENGING PATHWAYS / RESPONSE TO OXIDATIVE STRESS			
Protein exclusively detected in Pachía in both B treatments			
B4FKV6	Zm00001d014341	Peroxidase 54	Response to oxidative stress. Peroxidase activity
TRANSCRIPTION AND TRANSLATION			
Protein exclusively detected in Pachía in 10 mM B			
A0A096RFR6	Zm00001d039518	Eukaryotic translation initiation factor 3 subunit A (eIF3a)	Translation initiation factor activity. Protein synthesis. Formation of cytoplasmic translation initiation complex
Transporter and transport processes			
Proteins exclusively detected in Pachía in both B treatments			
A0A1D6EU13	Zm00001d006238	Calcium lipid binding protein-like	Lipid transport
A0A1D6JN64	Zm00001d027580	Outer mitochondrial membrane porin1 (ommp1)	Voltage-gated anion channel activity. Inorganic anion transport, transmembrane transport, anion transmembrane transport
Protein exclusively detected proteins in Sama in both B treatments			
Q7Y1W6	Zm00001d018693	Pentatricopeptide repeat 2 (PPR2)	Chloroplast translation
Unknown or not well determined			
Protein exclusively detected proteins in Sama in both B treatments			
A0A1D6DWG9	Zm00001d002089	Tetratricopeptide repeat (TPR)-like superfamily protein	Unknown

 doi:10.20944/preprints202305.0301.v1

[1]Proteins ID, Protein identification number in the UniProt database. [2]Gene Name, name or ID number of the corresponding gene of the identified protein as searched in the Maize Genetics and Genomics Database (MaizeGDB; https://www.maizegdb.org/). [3]Function/Biological process, annotated biological functions or biological process based on different databases. For more details, see Materials and Methods.

3. Discussion

Although 2793 proteins were detected in this proteomic analysis, only 303 proteins were differentially accumulated (Tables S1a and S2), which were classified into 26 functional categories. Functional analysis indicated that pathways involved in transcription and translation processes, amino acids metabolism, photosynthesis, carbohydrate metabolism, protein degradation, and protein stabilization and folding were highly enriched categories in both landraces (Figure 2). Remarkably, the expression levels of proteins related to these enriched processes were significantly different between Pachía and Sama.

3.1. Several proteases and translation-related proteins would allow Pachía to survive in media with B excess

Pachía is a B-sensitive maize cultivar described by Mamani-Huarcaya et al. [27]. Interestingly, the highest number of differentially accumulated proteins (DAPs) was found in the comparison group P10/P0.05 (Figure 1) suggesting that the B toxicity damage caused in Pachía could be partially relieved by these proteins. A remarkable number of these DAPs included in the categories of protein degradation (11), and transcription and translation (15) were strongly overexpressed in Pachía (Table S2 and 3). However, only four proteins of the transcription and translation group were markedly induced by 10 mM B in Sama (Table 4). The B-sensitive *Citrus grandis* had a higher number of proteins involved in protein degradation that was also overexpressed under B toxicity conditions in comparison with B-tolerant *Citrus sinensis* [36]. These authors concluded that B toxicity caused greater protein damage and proteolysis in *C. grandis*. Therefore, the high number of protein degradation-related proteins that were overexpressed in Pachía in 10 mM B would suggest that B toxicity would cause greater damage in Pachía proteins than in those of Sama leading to increased proteolysis in B-sensitive Pachía. Proteins related to protein degradation strongly overexpressed in Pachía included, among others, cysteine protease14 and four serine proteases (Table 3). Proteases have been implicated in plant acclimation to abiotic stress, playing a major role in the degradation of damaged and misfolded proteins, thus contributing to cell survival. In fact, cysteine and serine proteases are involved in degradation of misfolded proteins and protection against abiotic stresses [37-40]. Hence, these five proteases could have a main role in the degradation of damaged and misfolded proteins in Pachía under excess B, contributing to maintaining the correct conformation of Pachía proteins and, therefore, to the survival of this landrace under this stressful condition. In addition, a noteworthy number of proteins involved in transcription and translation processes were overexpressed at 10 mM B in Pachía, namely, 30 in contrast to only nine of Sama (Table S2). Proteomic analysis performed with dehydration, salt, and temperature stresses in cereals also displayed alterations in the levels of translation-related proteins, such as initiation factors and the ribosome constituent proteins [41 and references therein]. Furthermore, it has been suggested that a B excess provokes inhibition of RNA-dependent processes, such as transcription and translation, owing to the ability of B to form complexes with ribose molecules [42]. In this regard, Tanaka et al. [43] have suggested that B or boric acid acts on the translation machinery likely forming complexes with *cis*-diol groups of rRNA and tRNA. In addition, it has currently been proposed that high-B stress enhances ribosome frequency on stop codons leading to a global ribosome stalling [44]. Consequently, the high contents of leaf-soluble B in Pachía seedlings subjected to 10 mM B reported by Mamani-Huarcaya et al. [27] would generate an increased formation of B complexes with *cis*-diol groups of RNA that would damage ribosomes leading to a drop in protein synthesis likely through a global ribosome stalling. The strong overexpression of several ribosomal proteins would maintain the Pachía ribosome stability in B toxicity (Tables S2 and 3). These results are consistent with those reported for rice, where several ribosomal protein large subunit genes were upregulated under temperature stress, suggesting that

 doi:10.20944/preprints202305.0301.v1

their encoded proteins might be involved in stress amelioration, likely maintaining the proper functioning of ribosomes [41]. Interestingly, the eukaryotic translation initiation factor 3 subunit A (eIF3a) was exclusively detected in B toxicity in Pachía (Table 6). These factors are one of the most significant components involved in plant protein synthesis and, specifically, rice eIF3A has been proposed to play an important role in different stresses [45]. Therefore, eIF3a would also help to alleviate the drop in protein synthesis in Pachía. Thereby, Pachía would partly ameliorate injuries caused by B toxicity on protein synthesis and ribosome by overexpressing a high number of transcription- and translation-related proteins, abolishing a non-viable reduction of transcription and translation processes.

3.2. Proteins that would confer Sama more B toxicity tolerance

Polyamine oxidase 1 (PAO1) is an interesting protein that was clearly up-accumulated in Sama when compared to Pachía at 10 mM B and was also strongly induced in Sama by B toxicity (Tables 4 and 5). This enzyme catalyzes the back conversion of spermine (Spm) to spermidine (Spd), and Spd to putrescine (Put) [46]. Maize polyamines play a crucial role in abiotic stress response [33]. In fact, it has been reported that Put protects the plant photosynthetic apparatus against several abiotic stresses [47]. Moreover, the conjugation of Put to PSII proteins may lead to the structural and functional stability of PSII [46,48]. Therefore, the over-accumulation of PAO1 in Sama plants subjected to B toxicity would generate an increase in Put levels that would protect their photosynthetic apparatus resulting in the higher P_N observed in Sama under this stress, as described by Mamani-Huarcaya et al. [27]. This finding is consistent with results reported for Karoon, a drought-tolerant maize cultivar. Pakdel et al. [46] proposed that higher expression of PAO genes and enzymatic polyamine oxidation activity would protect the photosynthetic apparatus of Karoon under water stress.

3.2.1. Lower repression of photosynthesis-related proteins would enhance the B-toxicity tolerance of Sama

Photosynthesis is one of the essential physiological processes affected by B toxicity [2,22]. Photosynthetic efficiency could be achieved in Sama under B toxicity conditions increasing the synthesis of photosynthetic pigments, since chlorophyll content is a major limiting component of the photosynthetic efficiency [49]. Interestingly, Sama had a strong over-accumulation of magnesium-chelatase subunit H1 chloroplastic (ChlH1) at 10 mM B in comparison with those from Pachía (Table 5). ChlH binds to porphyrin and catalyzes the insertion of Mg^{2+} into protoporphyrin IX [50]. Accordingly, the over-accumulation of ChlH1 in Sama would explain its higher contents of chlorophyll a in B toxicity and the higher P_N described by Mamani-Huarcaya et al. [27].

In this study, 25 proteins related to photosynthetic light reactions were differentially accumulated, most of them involved in electron transport, light harvesting, and oxygen evolving processes (Table S2). Pachía and Sama presented several photosynthesis-related proteins that were repressed by B toxicity when their expressions were compared with those of Pachía and Sama, respectively, in media with 0.05 mM B (Table S2). However, the number of these DAPs was lower in Sama than in Pachía (11 versus 16, respectively; Table S2) and, besides, those proteins commonly down-accumulated in both landraces had a weaker decrease in Sama (Table 2). In addition, only two photosynthetic proteins were strongly down-expressed 3-fold or more (corresponding to FC≤ 0.33) by B toxicity in Sama in contrast to ten proteins found in Pachía (Tables 3 and 4). This decreased accumulation of photosynthesis related-proteins may cause lower photosynthetic performance in B-toxicity-treated Pachía plants than in Sama plants, as described by Mamani-Huarcaya et al. [27]. Therefore, Sama would retain sufficient levels of photosynthesis-related proteins in 10 mM B, which would allow it to maintain photosynthetic parameters at similar levels to those of the control conditions, as reported by Mamani-Huarcaya et al. [27]. Furthermore, three photosynthesis-related proteins were up-accumulated in Sama when their expressions were compared with those of Pachía in 10 mM B, namely, oxygen-evolving enhancer protein 2-1 chloroplastic (OEE2-1), post-illumination chlorophyll fluorescence increase (ZmPIFI), and NAD(P)H-quinone oxidoreductase subunit S chloroplastic (NDHS) (Tables 5 and S2). OEE2-1 is likely an extrinsic protein of the oxygen-evolving

complex (OEC) (UniProt; https://www.uniprot.org/). The OEC is stabilized and protected by extrinsic polypeptides [51]. The strong OEE2-1 over-accumulation in 10 mM B in Sama could facilitate the stability and protection of the OEC leading to the higher photosynthetic electron transporter rate (ETR) observed in this landrace [27]. Regarding ZmPIFI, it is homologous to the PIFI protein of *Arabidopsis thaliana* (AtPIFI), an essential component of the NAD(P)H dehydrogenase (NDH) complex involved in chlororespiratory electron transport around PSI [52]. The *Atpifi* mutant had a lower nonphotochemical quenching (NPQ) than wild type under high light irradiances, suggesting that AtPIFI would protect plants from photooxidative stress triggered by excessive light [52]. Consequently, both ZmPIFI over-accumulation and the higher NPQ values that Sama showed in 10 mM B, unlike those from Pachía (Table 5; [27]), suggest that ZmPIFI would also be a component of the maize NDH complex playing a role in oxidative photoprotection of this landrace under B-toxicity conditions. Furthermore, unlike Sama, several subunits of the NDH complex were markedly repressed in Pachía by B toxicity (Tables S2, 3, and 4). The NDH complex mediates cyclic electron transport around PSI playing a crucial role in C_4 photosynthesis [53,54]. NDH-mediated cycle electron transport (NDH-CET) performs two functions: 1) maintaining photosynthetic redox balance in the electron transfer avoiding stromal overreduction and functioning as a safety valve for excess electrons under stress, and 2) supplying ATP for efficient carbon assimilation, especially under stressful conditions [53-56]. The finding that none of the above components of the NDH complex was significantly repressed by B-toxicity in Sama suggests that its NDH-CET would prevent stromal overreduction and would protect against photooxidation. This fact would explain the high values of net photosynthetic CO_2 assimilation (P_N), maximum photochemical efficiency (Fv'/Fm'), and quantum yield efficiency of PSII electron transport (Φ_{PSII}) reported in Sama at 10 mM B, which were similar to those of control conditions [27]. Consistent with our data, Zhu et al. [56] have suggested that an increased abundance of NDH subunits in salt-stressed wheat would enhance NDH-CET alleviating the accumulation of excess electrons and maintaining energy homeostasis. Moreover, the subunit S of the NDH complex was over-accumulated in Sama under B toxicity when compared to those from Pachía, leading to a likely higher amount of NDH-complex that would provide extra ATP to achieve better P_N and growth at this landrace in media with 10 mM B as, in fact, was observed by Mamani-Huarcaya et al. [27]. In addition, a higher supply of ATP could be obtained in Sama in comparison to Pachía under B toxicity from a weaker decrease of the α- and β-chloroplastic subunits of ATP synthase in Sama (Table 2). Although B excess causes photosynthetic damage [2,22], plants have evolved mechanisms to repair these injuries that require a high amount of ATP from chloroplastic ATP synthase [57,58]. In Sama, B toxicity barely affected photosynthetic parameters [27]. This finding points out that this landrace would own mechanisms to repair its photosynthetic machinery. Likely, one of these mechanisms would be to provide greater ATP availability, which would be achieved by maintaining sufficient levels of NDH and ATP synthase complexes that would synthesize the amounts of ATP needed to repair its photosynthetic machinery and, therefore, to maintain its photosynthetic values at levels similar to those of control conditions.

4. Materials and Methods

4.1. Plant materials and growth conditions

Sama and Pachía, two Peruvian maize landraces from the Sama valley and the Pachía district (to the east of Tacna), were used in this study. Seeds were surface-sterilized as described by Mamani-Huarcaya et al. [27]. Afterwards, the seeds were placed in seedbeds filled with a perlite/vermiculite mixture (1/1, v/v) and watered with deionized H_2O. After seven days, seedlings were transplanted to 30-L plastic containers with a nutrient solution (NS) that was identical to the one used by Mamani-Huarcaya et al. [27]. After two days of acclimation to hydroponic medium, the seedlings were divided into groups and transferred to fresh NS supplemented with 10 mM H_3BO_3 (B toxicity conditions) or 0.05 mM H_3BO_3 (control conditions). This medium was aerated by air pumps and renewed twice a week. The seedlings were germinated and grown hydroponically in a growth chamber under a 12 h light/12 h dark regime (215 µmol m^{-2} s^{-1} of photosynthetically active radiation at plant height), at 22ºC and 50% relative humidity. The plants were randomly harvested 10 days after the onset of the B

 doi:10.20944/preprints202305.0301.v1

treatments and their leaves were quickly separated with a scalpel, frozen in liquid nitrogen and stored at –80°C until further analysis.

4.2. Protein extraction and digestion

Maize leaves (200-250 mg fresh weight) from four separate seedlings per condition (B treatment and maize landrace) were ground to a fine powder in a mortar precooled with liquid nitrogen. Proteins were extracted with trichloroacetic acid (TCA)/acetone-phenol [59], solubilized in a solution containing 7 M urea, 2 M thiourea and 2% (w/v) CHAPS (3 [(3-cholamidopropyl) dimethylammonium]-1-propanesulfonate), and quantified by the Bradford method using bovine serum albumin (BSA) as a standard [60].

The cleaning of maize protein extract, protein digestion, and mass spectrometry determinations were carried out at the Proteomics Facility for Research Support Central Service (SCAI) of the University of Córdoba (Spain) as follows.

Biological quadruplicate samples were separated and cleaned as described. Leaf protein extracts (50 µg of BSA protein equivalents per sample) were electrophoretically pre-concentrated in a centimeter band of 10% (w/v) SDS-PAGE gel. Protein bands were excised from the gels and, afterwards, the gel pieces were distained in 200 mM ammonium bicarbonate/50% acetonitrile for 15 min, followed by 5 min in 100% acetonitrile. Proteins were reduced by addition of 20 mM dithiothreitol in 25 mM ammonium bicarbonate and incubated for 20 min at 55 °C. The mixture was cooled to room temperature and then free thiols were alkylated by adding 40 mM iodoacetamide in 25 mM ammonium bicarbonate for 20 min in the dark. Finally, the gel pieces were washed twice in 25 mM ammonium bicarbonate.

Proteolytic digestion was performed by addition of trypsin to a final concentration of 12.5 ng/µL in 25 mM ammonium bicarbonate at 37 ºC overnight. Protein digestion was stopped by adding trifluoroacetic acid at a final concentration of 1% (v/v). Finally, the digested samples were vacuum-dried and dissolved in a mixture of 2% (v/v) acetonitrile and 0.05% (v/v) trifluoroacetic acid.

4.3. Shotgun-DDA-LC-MS/MS analysis

Peptide separations were performed on a nano-LC using Dionex Ultimate 3000 nano UPLC (Thermo Scientific, San Jose, CA, USA), equipped with a C18 75 µm × 50 cm Acclaim Pepmap column (Thermo Scientific, San Jose, CA, USA), at 40 °C at a flow rate of 300 nL/min. Peptide mixtures were previously concentrated and cleaned up on a 300 µm x 5 mm Acclaim Pepmap precolumn (Thermo Scientific, San Jose, CA, USA) using 2% acetonitrile/0.05% trifluoroacetic acid at 5 µL/min for 5 min. Peptides were eluted with a gradient of 60 min ranging from 96% solvent A (0.1% formic acid) to 90% solvent B (80% acetonitrile and 0.1% formic acid), followed by an 8 min wash at 90% solvent B and a 12 min re-equilibration at 4% solvent B. Eluted peptides were converted to gas-phase ions by nanoelectrospray ionization and analyzed on a Thermo Orbitrap Fusion mass spectrometer (Thermo Scientific, San Jose, CA, USA) operated in the positive mode. Survey scans of peptide precursors were acquired over the m/z range 400−1500 at 120K resolution (at 200 m/z) with a 4×10^5 ion count target. Tandem MS was performed by isolation at 1.2 Da with the quadrupole. Monoisotopic precursor ions were fragmented by CID (Chemically Induced Dimerization) in the ion trap, which was set up as follows: automatic gain control, 2×10^3; maximum injection time, 50 ms; and normalized collision energy of 35%. Only those precursors with charge state 2–5 were sampled for MS2. A dynamic exclusion time of 15 s and a tolerance of 10 ppm around the selected precursor and its isotopes were used to avoid redundant fragmentations. The instrument was run in top 30 mode with 3-s cycles, meaning the instrument would continuously perform MS2 events until a maximum of top 30 non-excluded precursors or 3 s, whichever was shorter.

4.4. Protein quantification

Charge state deconvolution and deisotoping were not performed. MS2 spectra were searched using MaxQuant software v. 1.5.7.4 [61]. MS2 spectra were searched with Andromeda

engines against a database of Uniprot *Zea mays*_Jun19. Peptides generated from tryptic digestion were searched employing the following parameters: up to one missed cleavage, carbamidomethylation of cysteines as fixed modifications, and oxidation of methionine as variable modifications. The precursor mass tolerance was 10 ppm and product ions were searched at 0.6 Da tolerances. A target-decoy search strategy was applied, which integrates multiple peptide parameters such as length, charge, number of modifications, and identification score into a single quality that acts as statistical evidence on the quality of each single peptide spectrum match. The identified peptides were grouped into proteins according to the law of parsimony and filtered to 1% false discovery rate (FDR). Peptide quantification was carried out using MaxQuant software, in a MaxLFQ label-free quantification method [62]. In the MaxLFQ label-free quantification method, a retention time alignment and identification transfer protocol ("match-between runs" feature inMaxQuant) was applied. Proteins identified from only one peptide were not taken into account in this analysis. Peak intensities across the whole set of quantitative data for all peptides in the samples were imported from the LFQ intensities of proteins from the MaxQuant analysis and normalized according to Cox et al. [62]. LFQ normalized intensity values were transformed to a logarithmic scale with base two. Protein quantification and calculation of statistical significance were carried out using Student-*t* test and error correction (P-value ≤ 0.05). The criteria used to consider a protein as differentially expressed were as follows: (a) the protein was consistently present in at least three biological replicates per condition; (b) it had statistically significant differences (Student-*t* test, $P \leq 0.05$) between genotypes or B treatments; and (c) a fold change ≥ 1.5 or ≤ 0.66667. The differentially accumulated proteins were manually categorized by function using different databases (Uniprot, https://www.uniprot.org/; Maize Genetics and Genomics, https://www.maizegdb.org/; ExplorEnz, https://www.enzyme-database.org/; BRENDA, https://www.brenda-enzymes.org/; KEGG: Kyoto Encyclopedia of Genes and Genomes, https://www.genome.jp/kegg/; and PANTHER: Protein ANalysis THrough Evolutionary Relationships, http://pantherdb.org/).

5. Conclusions

Overexpression of several proteases and transcription- and translation-related proteins would allow Pachía to degrade and replace partially the proteins damaged by B toxicity achieving survival under this stress condition.

In Sama, PAO1 over-accumulation and weaker knockdown of several subunits of NDH and ATP synthase complexes under B excess would confer a greater B toxicity tolerance to this landrace by: 1) acting as an electron safety valve that would avoid stromal overreduction, and thus decrease photosynthetic damage and, 2) providing an additional supply of ATP that would contribute to repair the photosynthetic system of Sama.

Supplementary Materials: Table S1a: Dataset of proteins identified by shotgun-DDA analysis; Table S1b: Dataset, statistical analysis and fold change of proteins identified by shotgun-DDA analysis; Table S2: Fold change ratios, *P*-values and statistical significances of all significantly accumulated proteins classified by functional categories.

Author Contributions: Plant growth and harvesting, and protein extraction and quantification, B.M.M.-H. with substantial contribution of M.T.N.-G. and J.R.; research planning and design, J.R. with the help of all authors; analysis and interpretation of data, J.R.; writing - first draft, J.R.; editing and review - second draft, J.R. and A.G.-F. All authors critically revised the manuscript and made significant contributions. All authors have read and agreed to the published version of the manuscript.

Funding: This research was funded by Agencia Andaluza de Cooperación Internacional para el Desarrollo (Consejería de Igualdad y Políticas Sociales) from Junta de Andalucía (2016SEC014), and by the Consejería de Economía, Innovación, Ciencia y Empleo from Junta de Andalucía (BIO-266).

Data Availability Statement: The data presented in this study are available in the text and supplemental data.

Acknowledgments: The authors would like to thank SCAI of the University of Córdoba (Spain) for protein identification and, especially, to Carlos Fuentes Almagro his skillful technical assistance.

Conflicts of Interest: The authors declare no conflict of interest. The funders had no role in the design of the study; in the collection, analyses, or interpretation of data; in the writing of the manuscript; or in the decision to publish the results.

References

1. Warington, K. The effect of boric acid and borax on the broad bean and certain other plants. *Ann. Bot.* **1923**, *37*, 629–672.
2. Princi, M.P.; Lupini, A.; Araniti, F.; Longo, C.; Mauceri, A.; Sunseri, F.; Abenavoli, M.R. Boron toxicity and tolerance in plants: recent advances and future perspectives. In *Plant Metal Interaction: Emerging Remediation Techniques*, Ahmad, P., Ed.; Elsevier Inc: Amsterdam, Netherlands, 2016; pp. 115–147.
3. González-Fontes, A.; Fujiwara, T. Advances in plant boron. *Int. J. Mol. Sci*. **2020**, *21*, 4107.
4. González-Fontes, A. Why boron is an essential element for vascular plants. *New Phytol*. **2020**, *226*, 1228–1230.
5. Wimmer, M.A.; Abreu, I.; Bell, R.W.; Bienert, M.D.; Brown, P.H.; Dell, B.; Fujiwara, T.; Goldbach, H.E.; Lehto, T.; Mock, H.-P.; et al. Boron: an essential element for vascular plants. *New Phytol*. **2020**, *226*, 1232–1237.
6. Ishii, T.; Matsunaga, T. Isolation and characterization of a boron-rhamnogalacturonan-II complex from cell walls of sugar beet pulp. *Carbohydr. Res*. **1996**, *284*, 1–9.
7. Kobayashi, M.; Matoh, T.; Azuma, J. Two chains of rhamnogalacturonan II are cross-linked by borate-diol ester bonds in higher plant cell walls. *Plant Physiol.* **1996**, *110*, 1017–1020.
8. O'Neill, M.A.; Warrenfeltz, D.; Kates, K.; Pellerin, P.; Doco, T.; Darvill, A.G.; Albersheim, P. Rhamnogalacturonan-II, a pectic polysaccharide in the walls of growing plant cell, forms a dimer that is covalently cross-linked by a borate ester. *J. Biol. Chem*. **1996**, *271*, 22923–22930.
9. Cakmak, I.; Römheld, V. Boron deficiency-induced impairments of cellular functions in plants. *Plant Soil* **1997**, *193*, 71–83.
10. Goldbach, H.E.; Yu, Q.; Wingender, R.; Schulz, M.; Wimmer, M.; Findeklee, P.; Baluška, F. Rapid response reactions of roots to boron deprivation. *J. Plant Nutr. Soil Sci*. **2001**, *164*, 173–181.
11. Brown, P.H.; Bellaloui, N.; Wimmer, M.A.; Bassil, E.S.; Ruiz, J.; Hu, H.; Pfeffer, H.; Dannel, F.; Römheld, V. Boron in plant biology. *Plant Biol*. **2002**, *4*, 205–223.
12. Voxeur, A.; Fry, S.C. Glycosylinositol phosphorylceramides from Rosa cell cultures are boron-bridged in the plasma membrane and form complexes with rhamnogalacturonan II. *Plant J*. **2014**, *79*, 139–149.
13. Wang, N.; Yang, C.; Pan, Z.; Liu, Y.; Peng, S. Boron deficiency in woody plants: various responses and tolerance mechanisms. *Front. Plant Sci*. **2015**, *6*, 916.
14. Blevins, D.G.; Lukaszewski, K.M. Boron in plant structure and function. *Annu. Rev. Plant Physiol. Plant Molec. Biol*. **1998**, *49*, 481–500.
15. Camacho-Cristóbal, J.J.; Navarro-Gochicoa, M.T.; Rexach, J.; González-Fontes, A.; Herrera-Rodríguez, M.B. Plant response to boron deficiency and boron use efficiency in crop plants. In *Plant Micronutrient Use Efficiency. Molecular and Genomic Perspectives in Crop Plants*, Hossain, M.A., Kamiya, T., Burritt, D.J., Phan Tran L.-S., Fujiwara. T., Eds.; Elsevier Inc., 2018; pp. 109–121.
16. Shireen, F.; Nawaz, M.A.; Chen, C.; Zhang, Q.; Zheng, Z.; Sohail, H.; Sun, J.; Cao, H.; Huang, Y.; Bie, Z. Boron: functions and approaches to enhance its availability in plants for sustainable agriculture. *Int. J. Mol. Sci*. **2018**, *19*, 1856.
17. Reid, R.J.; Hayes, J.E.; Post, A.; Stangoulis, J.C.R.; Graham, R.D. A critical analysis of the causes of boron toxicity in plants. *Plant Cell Environ*. **2004**, *27*, 1405–1414.
18. Camacho-Cristóbal, J.J.; Rexach, J.; González-Fontes, A. Boron in plants: deficiency and toxicity. *J. Integr. Plant Biol*. **2008**, *50*, 1247–1255.
19. Beato, V.M.; Rexach, J.; Navarro-Gochicoa, M.T.; Camacho-Cristóbal, J.J.; Herrera-Rodríguez, M.B.; Maldonado, J.M.; González-Fontes, A. A tobacco asparagine synthetase gene responds to carbon and nitrogen status and its root expression is affected under boron stress. *Plant Sci*. **2010**, *178*, 289–298.
20. Beato, V.M.; Navarro-Gochicoa, M.T.; Rexach, J.; Herrera-Rodríguez, M.B.; Camacho-Cristóbal, J.J.; Kempa, S.; Weckwerth, W.; González-Fontes, A. Expression of root glutamate dehydrogenase genes in tobacco plants subjected to boron deprivation. *Plant Physiol. Biochem*. **2011**, *49*, 1350–1354.
21. Liu, X.; Zhang, J.-W.; Guo, L.-X.; Liu, Y.-Z.; Jin, L.-F.; Hussain, S.B.; Du, W.; Deng, Z.; Peng, S.-A. Transcriptome changes associated with boron deficiency in leaves of two citrus scion-rootstock combinations. *Front. Plant Sci*. **2017**, *8*, 317.
22. Landi, M.; Margaritopoulou,T.; Papadakis, I.E.; Araniti, F. Boron toxicity in higher plants: an update. *Planta* **2019**, *250*, 1011–1032.
23. Brdar-Jokanovi´c, M. Boron toxicity and deficiency in agricultural plants. *Int. J. Mol. Sci*. **2020**, *21*, 1424.
24. Kabay, N.; Güler, E.; Bryjak, M. Boron in seawater and methods for its separation—a review. *Desalination* **2010**, *261*, 212–217.

25. Chatzistathis, T.; Fanourakis, D.; Aliniaeifard, S.; Kotsiras, A.; Delis, C.; Tsaniklidis, G. Leaf age-dependent effects of boron toxicity in two *Cucumis melo* varieties. *Agronomy*. **2021**, *11*, 759.
26. Uluisik, I.; Karakaya, H.C.; Koc, A. The importance of boron in biological systems. *J. Trace Elem. Med. Biol.* **2018**, *45*, 156–162.
27. Mamani-Huarcaya, B.M.; González-Fontes, A.; Navarro-Gochicoa, M.T.; Camacho-Cristóbal, J.J.; Ceacero, C.J.; Herrera-Rodríguez, M.B.; Fernández Cutire, Ó.; Rexach, J. Characterization of two Peruvian maize landraces differing in boron toxicity tolerance. *Plant Physiol. Biochem*. **2022**, *185*, 167–177.
28. Behera, B.; Kancheti, M.; Raza, M.B.; Shiv, A.; Mangal, V.; Rathod, G.; Altaf, M.A.; Kumar, A.; Aftab, T.; Kumar, R.; et al. Mechanistic insight on boron-mediated toxicity in plant *vis*-a-*vis* its mitigation strategies: a review. *Int. J. Phytoremediat*. **2023**, *25*, 9-26.
29. Ralston, N.V.C.; Hunt, C.D. Diadenosine phosphates and *S*-adenosylmethionine: novel boron binding biomolecules detected by capillary electrophoresis. *Biochim. Biophys. Acta* **2001**, *1527*, 20–30.
30. Liang, Z.; Pandey, P.; Stoerger, V.; Xu, Y.; Qiu, Y.; Ge, Y.; Schnable, J.C. Conventional and hyperspectral timeseries imaging of maize lines widely used in field trials. *GigaScience* **2018**, *72*, 1–11.
31. Andorf, C.; Beavis, W.D.; Hufford, M.; Smith, S.; Suza, W.P.; Wang, K.; Woodhouse, M.; Yu, J.; Lübberstedt, T. Technological advances in maize breeding: past, present, and future. *Theor. Appl. Genet*. **2019**, *132*, 817-849.
32. Kausch, A.P.; Wang, K.; Kaeppler, H.F.; Gordon-Kamm, W. Maize transformation: history, progress, and perspectives. *Mol. Breed*. **2021**, *41*, 38.
33. Xi, Y.; Hu, W.; Zhou, Y.; Liu, X.; Qian, Y. Genome-wide identification and functional analysis of polyamine oxidase genes in maize reveal essential roles in abiotic stress tolerance. *Front. Plant Sci*. **2022**, *13*, 950064.
34. Ogunwole, A.A.; Otusanya, O.O.; Oloyede, F.A.; Olabamiji, T.M. Comparative effects of boron toxicity and deficiency on the growth, chlorophyll, protein and some cations accumulation in *Zea mays* seedlings. *Int. J. Sci. Res. Innov*. **2015**, 17, 316–335.
35. Gotz, L.F.; Silvestrin, F.; Motta, A.C.V.; Pauletti, V. Response to application and tissue diagnosis of boron deficiency and toxicity in maize. *Commun. Soil Sci. Plant Anal*. **2021**, *52:22*, 2898–2911.
36. Sang, W.; Huang, Z.-R.; Yang, L.-T.; Guo, P.; Ye, X.; Chen, L.-S. Effects of high toxic boron concentration on protein profiles in roots of two citrus species differing in boron-tolerance revealed by a 2-DE based MS approach. *Front. Plant Sci*. **2017**, *8*, 180.
37. Fan, T.; Bykova, N.V.; Rampitsch, C.; Xing, T. Identification and characterization of a serine protease from wheat leaves. *Eur. J. Plant Pathol*. **2016**, *146*, 293–304.
38. Malefo, M.B.; Mathibela, E.O.; Crampton, B.G.; Makgopa, M.E. Investigating the role of Bowman-Birk serine protease inhibitor in Arabidopsis plants under drought stress. *Plant Physiol. Biochem*. **2020**, *149*, 286–293.
39. D'Ippolito, S.; Rey-Burusco, M.F.; Feingold, S.E.; Guevara, M.G. Role of proteases in the response of plants to drought. *Plant Physiol. Biochem*. **2021**, *168*, 1–9.
40. Sharma, P.; Gayen, D. Plant protease as regulator and signaling molecule for enhancing environmental stress-tolerance. *Plant Cell Reports*. **2021**, *40*, 2081–2095.
41. Moin, M.; Bakshi, A.; Saha, A.; Dutta, M.; Madhav, S.M.; Kirti, P.B. Rice ribosomal protein large subunit genes and their spatio-temporal and stress regulation. *Front. Plant Sci*. **2016**, *7*, 1284.
42. Nozawa, A.; Miwa, K.; Kobayashi, M.; Fujiwara, T. Isolation of *Arabidopsis thaliana* cDNAs that confer yeast boric acid tolerance. *Biosci. Biotechnol. Biochem*. **2006**, *70*, 1724–1730.
43. Tanaka, M.; Sotta, N.; Yamazumi, Y.; Yamashita, Y.; Miwa, K.; Murota, K.; Chiba, Y.; Hirai, M.Y.; Akiyama, T.; Onouchi, H.; et al. The minimum open reading frame, AUG-stop, induces boron-dependent ribosome stalling and mRNA degradation. *Plant Cell* **2016**, *28*, 2830–2849.
44. Sotta, N.; Chiba, Y.; Miwa, K.; Takamatsu, S.; Tanaka, M.; Yamashita, Y.; Naito, S.; Fujiwara, T. Global analysis of boron-induced ribosome stalling reveals its effects on translation termination and unique regulation by AUG-stops in Arabidopsis shoots. *Plant J*. **2021**, *106*, 1455–1467.
45. Saidi, A.; Hajibarat, Z. In-silico analysis of eukaryotic translation initiation factors (eIFs) in response to environmental stresses in rice (*Oryza sativa*). *Biologia* **2020**, *75*, 1731–1738.
46. Pakdel, H.; Hassani, S.B.; Ghotbi-Ravandi, A.A.; Bernard, F. Contrasting the expression pattern change of polyamine oxidase genes and photosynthetic efficiency of maize (*Zea mays* L.) genotypes under drought stress. *J. Biosci*. **2020**, *45*, 73.
47. Shu, S.; Guo, S.-R.; Sun, J.; Yuan, L.-Y. Effects of salt stress on the structure and function of the photosynthetic apparatus in *Cucumis sativus* and its protection by exogenous putrescine. *Physiol. Plant*. **2012**, *146*, 285–296.
48. Hamdani, S.; Yaakoubi, H.; Carpentier, R. Polyamines interaction with thylakoid proteins during stress. *J. Photochem. Photobiol. B-Biol*. **2011**, *104*, 314–331.
49. Chen, M.; Blankenship, R.E. Expanding the solar spectrum used by photosynthesis. *Trends Plant Sci*. **2011**, *16*, 427–431.

50. Zhang, D.; Chang, E.; Yu, X.; Chen, Y.; Yang, Q.; Cao, Y.; Li, X.; Wang, Y.; Fu, A.; Xu, M. Molecular characterization of magnesium chelatase in soybean [*Glycine max* (L.) Merr.]. *Front. Plant Sci*. **2018**, *9*, 720.
51. Sasi, S.; Venkatesh, J.; Daneshi, R.F.; Gururani, M.A. Photosystem II extrinsic proteins and their putative role in abiotic stress tolerance in higher plants. *Plants*, **2018**, *7*, 100.
52. Wang, D.; Portis, A.R. A novel nucleus-encoded chloroplast protein, PIFI, is involved in NAD(P)H dehydrogenase complex-mediated chlororespiratory electron transport in Arabidopsis. *Plant Physiol*. **2007**, *144*, 1742–1752.
53. Ishikawa, N.; Takabayashi, A.; Noguchi, K.; Tazoe, Y.; Yamamoto, H.; von Caemmerer, S.; Sato, F.; Endo, T. NDH-mediated cyclic electron flow around photosystem I is crucial for C_4 photosynthesis. *Plant Cell Physiol*. **2016**, *57*, 2020–2028.
54. Ma, M.; Liu, Y.; Bai, C.; Yong, J.W.H. The significance of chloroplast NAD(P)H dehydrogenase complex and its dependent cyclic electron transport in photosynthesis. *Front. Plant Sci*. **2021**, *12*, 661863.
55. Yamori, W.; Shikanai, T. Physiological functions of cyclic electron transport around photosystem I in sustaining photosynthesis and plant growth. *Annu. Rev. Plant Biol*. **2016**, *67*, 81–106.
56. Zhu, D.; Luo, F.; Zou, R.; Liu, J.; Yan, Y. Integrated physiological and chloroplast proteome analysis of wheat seedling leaves under salt and osmotic stresses. *J. Proteomics* **2021**, *234*, 104097.
57. Murata, N.; Nishiyama, Y. ATP is a driving force in the repair of photosystem II during photoinhibition. *Plant Cell Environ*. **2018**, *41*, 285–299.
58. Araniti, F.; Miras-Moreno, B.; Lucini, L.; Landi, M.; Abenavoli, M.R. Metabolomic, proteomic and physiological insights into the potential mode of action of thymol, a phytotoxic natural monoterpenoid phenol. *Plant Physiol. Biochem*. **2020**, *153*, 141–153.
59. Wang, W.; Vignani, R.; Scali, M.; Cresti, M. A universal and rapid protocol for protein extraction from recalcitrant plant tissues for proteomic analysis. *Electrophoresis* **2006**, *27*, 2782–2786.
60. Bradford, M.M. A rapid and sensitive method for the quantitation of microgram quantities of proteins utilizing the principle of protein-dye binding. *Anal. Biochem*. **1976**, *72*, 248–254.
61. Cox, J.; Mann, M. MaxQuant enables high peptide identification rates, individualized p.p.b.-range mass accuracies and proteome-wide protein quantification. *Nat. Biotechnol*. **2008**, *26*, 1367–1372.
62. Cox, J.; Hein, M.Y.; Luber, C.A.; Paron, I.; Nagaraj, N.; Mann, M. Accurate proteome-wide label-free quantification by delayed normalization and maximal peptide ratio extraction, termed MaxLFQ. *Mol. Cell. Proteomics* **2014**, *13*, 2513–2526.